Effect of tensile stress on hydrogen permeation in 13% Cr super martensitic stainless steel

Anna Smirnova, anna.smirnova@ntnu.no
Roy Johnsen, roy.johnsen@ntnu.no
Kemal Nisancioglu, kemal.nisancioglu@material.ntnu.no
Norwegian University of Science and Technology, Trondheim/Norway

New equipment for investigation of hydrogen diffusion at different temperatures, mechanical stresses and hydrostatic pressures has been developed. This equipment can realistically simulate subsea conditions and the hydrogen diffusion measurement is based on the Devanathan-Stachurski permeation method. Hydrogen diffusion was studied in 13% Cr super martensitic stainless steel at 0%, 50%, 80% and 100% of the yield stress. Hydrogen diffusion coefficient increased moderately with mechanical stress due to deformation induced martensitic transformation. Effective sub-surface hydrogen concentration did not vary with tensile stress.

Key words: cathodic protection, hydrogen diffusion, tensile stress, stainless steel

Introduction

Hydrogen induced failures of subsea oil and gas production systems cause severe problems to both oil and gas companies and the environment [1]. Hydrogen becomes produced on the surface due to the cathodic protection system, becomes partly absorbed by the material and diffuses into the bulk of the material. This can lead to cracking caused by hydrogen in the components made of such materials as duplex stainless steels, martensitic stainless steels and nickel alloys [2-4]. The mechanisms of hydrogen embrittlement are not fully understood and there is a constant need for new testing methods [5, 6] and data in order to implement robust requirements in standards for materials for subsea applications.

Hydrogen embrittlement occurs as a synergistic effect of environmental parameters (hydrogen produced by cathodic protection, corrosion reaction and products and welding process), susceptible material (e.g. martensitic stainless steel) and mechanical stress (tensile, cyclic and residual stresses). Deformation of the material under mechanical stress has a significant effect on hydrogen diffusion, and it is therefore an important factor causing hydrogen cracking [7]. Subsea installations and components are normally protected cathodically. They are subject to deformation in installation and use, and they bear high mechanical loads. Hydrogen diffuses to areas with high stress intensity and accumulates in dislocations and other defects, in particular, at the crack tip where the stress intensity is very high [8]. This degrades the mechanical properties of the material and causes cracking at much lower stresses than anticipated from the nominal mechanical properties of a component.

Several authors have used the Devanathan-Stachurski hydrogen permeation method to study the influence of mechanical load on hydrogen diffusion in different types of steels. Huang et al. [9] and Chen et al. [10] studied hydrogen diffusion and concentration in iron and duplex stainless steels undergone plastic deformation. Both studies found that tensile stress decreased the hydrogen diffusion coefficient, while it increased hydrogen concentration in these materials. The decrease of diffusion coefficient was explained by nucleation of dislocations which act as traps and retard hydrogen diffusion. The increase in hydrogen concentration was attributed to the increased electrochemical production and absorption of hydrogen atoms due to an increase in the number of active sites on a deformed surface [9]. In nickel-based alloys undergone deformation, hydrogen permeation was increased due to formation of gliding dislocations that transport hydrogen atoms [11]. Several studies [9, 12] showed that elastic stress did not have any influence on hydrogen diffusion. The effect of mechanical load on hydrogen diffusivity and permeability in different types of steels is not yet fully understood and needs further investigation.

Hesjevik and Olsen [13] reported failures in 13% Cr super martensitic stainless steel pipelines caused by hydrogen. Little information about the effect of strain on hydrogen diffusivity in martensitic steels is available in the literature. Thus, the objective of this work was to study the effect of tensile stresses on hydrogen permeation in 13% Cr super martensitic stainless steels.

Experimental

Materials

The test material used in this work was low carbon 13% Cr super martensitic stainless steel (SMSS) supplied by TenarisNKKTubes[1]. The chemical composition of the material is shown Table 1. The area fraction of precipitated austenite in the microstructure was 19% as measured by Electron Back Scattered Diffraction (EBSD). The mechanical properties determined by destructive testing are shown in Table 2, and the stress-strain curve for the test material is shown in Fig. 1. It can be seen from this curve that the yield strength corresponds to 0.4% strain.

Table 1. *Chemical composition of 13% Cr SMSS test material.*

Alloy	Alloying element (wt%)							
	Cr	Ni	Mo	C	N	Mn	Si	Fe
13% Cr SMSS	12.30	5.90	2.15	0.01	0.014	-	-	Bal.

Table 2. *Mechanical properties of the 13% Cr super martensitic stainless steel test material.*

Alloy	Mechanical properties	
	Yield strength, MPa	Tensile strength, MPA
13% Cr SMSS	570	844

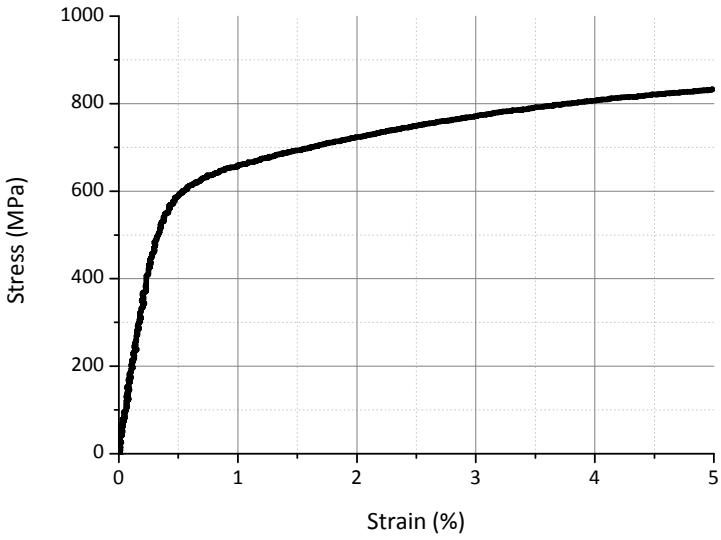

Figure 1. *Stress-strain curve obtained after destructive testing of the actual test material.*

The area fraction of the austenite phase in the samples, determined by electron back scatter diffraction (EBSD) analysis, was 18.7 ± 0.5 and 2.7 ± 0.5% for the as-received material and after deformation of the material by 0.4%, respectively. The values are based on measurements performed at three locations of each sample condition.

The test section of the tensile specimens was machined from one side, as shown in Fig. 2, and ground with 220 grit SiC paper from both sides to a final thickness of 300

[1] TenarisNKKTubes, 1-10 Minamiwatarida, Kawasaki City Kanagawa Prefecture, 210-0855, Japan

µm to obtain the membrane needed for the hydrogen permeation experiment to be described in the next section. The machined geometry also made possible theoretical calculation of the stress distribution in the test section, as will be described in the next section. The machined side was used for electrolytic charging of hydrogen for the purpose of hydrogen ingress into the sample.

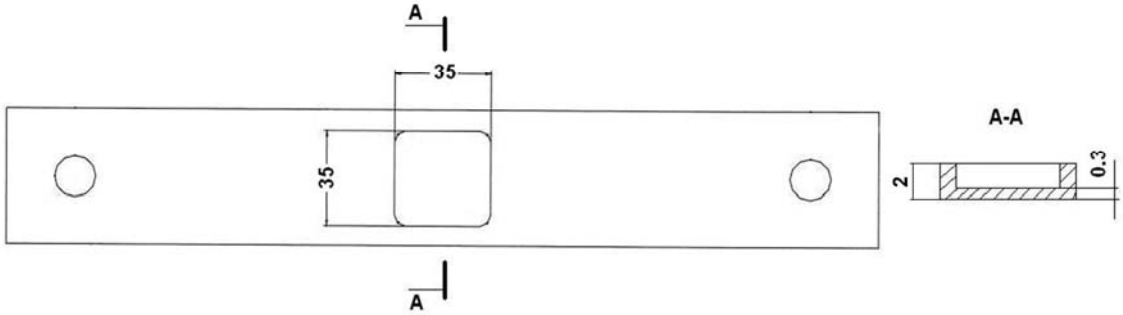

Figure 2. *Specimen.*

Method and Apparatus

The method used in this work for measuring the bulk diffusion coefficient and subsurface concentration of hydrogen was electrochemical hydrogen permeation [14] as described in ISO 17081:2004 [15]. The machined thin area of the specimen described above, acting as a membrane, was placed between two electrochemical cells that were electrically isolated from each other. In one cell (charging cell) a cathodic potential was applied to the specimen, ***e.g.***, -1050 mV vs. Ag/AgCl to simulate cathodic protection, in 3.5% NaCl solution. Hydrogen atoms formed by the reduction of water adsorbed on the specimen surface, and some of these became absorbed and diffused into the material. In the other cell (oxidation cell), which contained 0.1M NaOH solution, a positive potential, normally +350 mV vs. Ag/AgCl, was applied to the specimen to oxidize the hydrogen atoms which reach the opposite surface of the steel membrane. In this way the flux of hydrogen atoms diffusing through the sample is measured electrochemically. The bulk diffusion coefficient of hydrogen in the material and the sub-surface hydrogen concentration on the entry side of the specimen can be obtained from the data [15].

New equipment, based on the Devanathan-Stachuski approach, was developed to study hydrogen diffusion under combined influence of temperature, mechanical stresses and hydrostatic pressures (Fig. 3). The equipment was designed by Cormet Testing Systems, Finland[2]. The equipment consists of a two compartment autoclave integrated with a loading unit that is capable of applying constant load, fatigue load and slow strain-rate to the specimen design described above. The capacity of the loading unit is 30 kN. For the test specimen design used, a maximum average stress level of about 600 MPa can be attained in the test area. The autoclaves can be cooled/heated in the range of 4-80ºC using a cooling/heating bath. The electrolyte in the autoclaves can be pressurized up to 100 bar with gas supplied from an external reservoir. Titanium autoclaves allow testing of a variety of corrosive media, ***e.g.***, electrolytes containing corrosive gases, such as CO_2, H_2S and oxygen. Both base

[2] www.cormet.fi

material and welded samples can be tested. The main features of the equipment are briefly summarized in Table 3.

1	Load cell	6	Dial indicator and limit switches
2	Pressure sensor	7	Gear box with worm gear
3	Upper specimen holder	8	Heating/cooling bath
4	Autoclave	9	Bobbling bottle
5	Lower specimen holder	10	Gas inlet pressure reducer

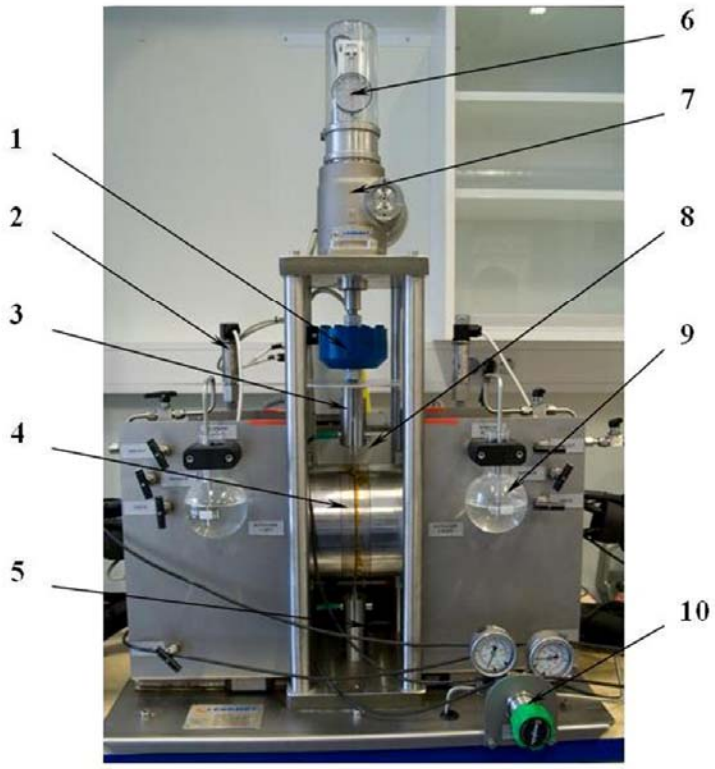

Figure 3. *General view of the equipment with the mail positions*.

Table 3. *Main features of the equipment.*

Loading unit capacity	30 kN
Load types	Constant, fatigue, slow strain-rate
Temperature	4-80 ºC
Pressure	Max. 100 bar
Ti-autoclaves	Variety of corrosive-media can be tested

One of the limitations of the equipment is the absence of a recirculation system. This limits the replacement of the electrolyte, which has to be done manually, to ambient pressures and temperatures.

In the present work, the electrolyte in the oxidation cell was purged with nitrogen gas for 1 hour prior to the test start and the autoclave was sealed so that no oxygen from external atmosphere could penetrate it. Magnetic stirrers were used in both cells at a speed of 500 rpm. The tests were carried out at 20 ± 0.5°C.

Procedure

Testing procedure consisted of alternating rising and decay transients (see Fig. 4). Initially, the potential -1050 mV vs. Ag/AgCl was applied to the cathode surface of the membrane at zero load, which gave a positive transient for the permeation flux of hydrogen into the specimen. When a steady-state permeation flux was attained, the potential on the charging side was increased to -550 mV vs. Ag/AgCl, which allowed all free hydrogen to diffuse out from the specimen, giving a decay transient in the flux. When the flux attained a low steady background value, the potential was again set at -1050 mV vs. Ag/AgCl, and a new permeation transient was measured. The value of the effective diffusion coefficient obtained from the first permeation transient was disregarded because this transient was affected by irreversible trapping. The subsequent transients were analysed with the assumption that all irreversible traps were occupied during the first diffusion run, and hydrogen diffusion was governed by lattice diffusion and reversible trapping. After the second decay transient was measured and the background current attained a low steady value, 50% of YS was applied to the specimen, and the specimen was at the same time polarized to -1050 mV vs. Ag/AgCl. The same procedure was repeated for 80% of YS and 100% of YS on the same sample, as sketched in Fig. 4

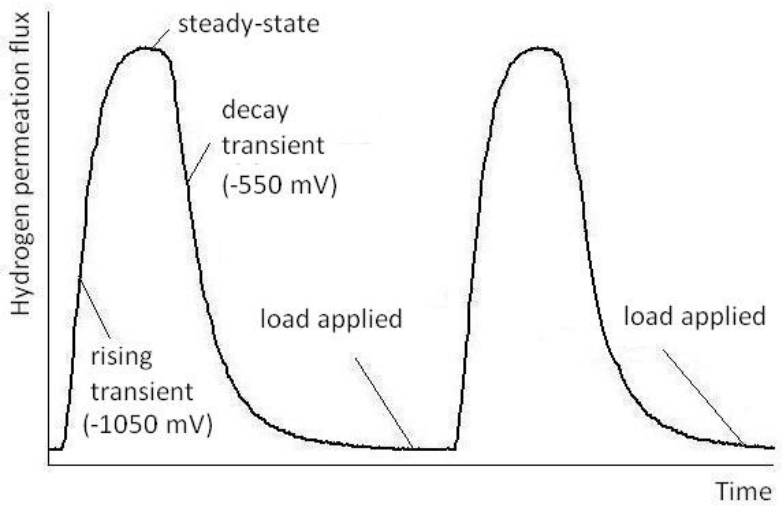

Figure 4. *Schematic illustration of the test procedure.*

Theoretical considerations

Stress distribution in the membrane test section

Tensile stress distribution in the membrane was simulated by use of software ABAQUS in order to correlate the true stress distribution in the membrane with the externally applied load. ABAQUS is a suit of software applications for finite element analysis and computer-aided engineering. An example of the numerical results for an applied load of 5 kN showed a nonuniform stress distribution (Fig. 5) with a maximum in the centre of the membrane and a minimum at the edge, which was 32% smaller than the maximum. The average stress in the membrane was then calculated and related to the net section stress (NSS) of the unmachined section of the sample, which in turn is related directly to the applied external load. The correlation is shown in Fig. 6. Using the figure and the mechanical properties of 13% Cr SMSS, the average stress values in the membrane, selected for the experiments, expressed in

terms of % YS (yield stress), were calculated as a function of applied load, as shown in Table 4.

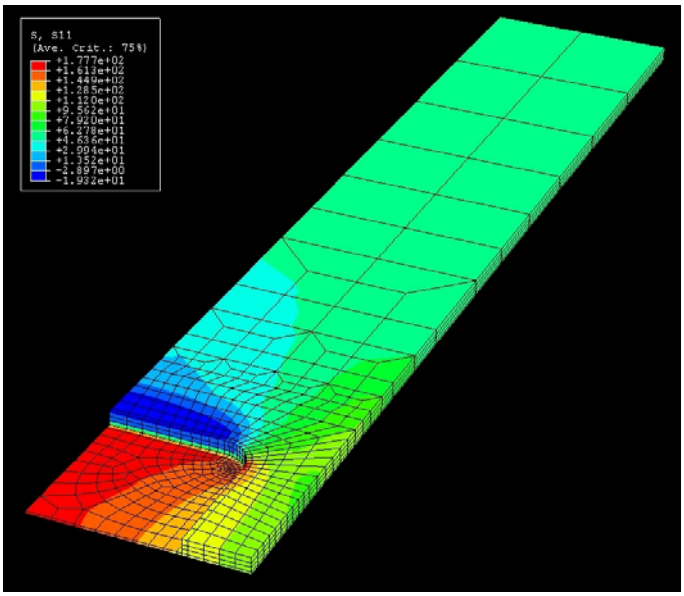

Figure 5. *Simulated stress distribution in the specimen at 5 kN applied load.*

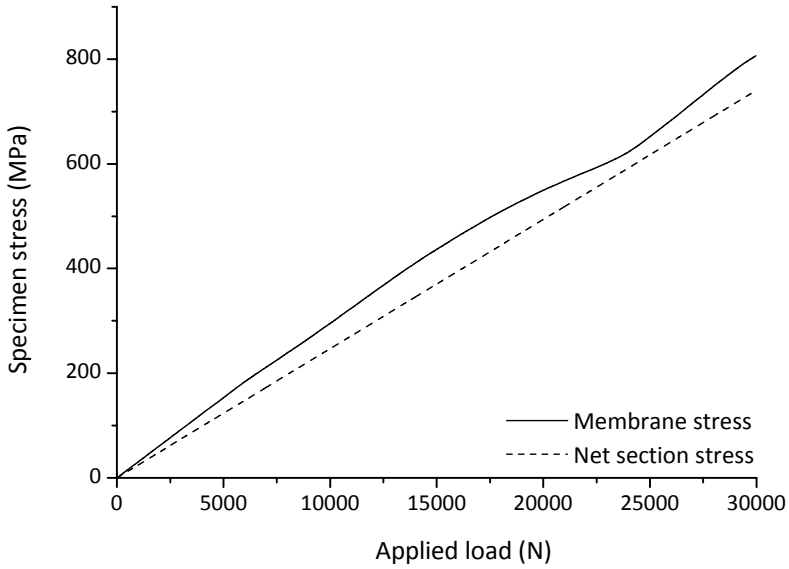

Figure 6. *Net section stress versus membrane stress.*

Table 4. *Load values for tested average membrane stresses.*

Average membrane stress, % of YS	Applied load on the specimen, N
50	8700
80	15700
100	21300

Hydrogen diffusion coefficient and sub-surface hydrogen concentration

The hydrogen diffusion coefficient determined from the flux transients in the conventional way, *e.g.*, the time lag method [15], would be an effective diffusion

coefficient D_{eff} because of the duplex martensite-austenite structure of the 13% Cr SMSS sample. Since only the martensite phase transports the hydrogen, the permeation flux is related to the sub-surface concentration of hydrogen C_0 according to the equation

$$\frac{i_{ss}}{F} = \frac{D_{eff}(1-\varphi_\gamma)C_0}{L} \quad (1)$$

where i_{ss} is steady-state permeation current density and F is Faraday's constant (96485 C/mol), φ_γ is the austenite area fraction, and L is the membrane thickness.

The area fraction of austenite φ_γ decreases with applied stress as indicated below. The correlation between φ_γ and tensile stress was obtained by extrapolating the experimental data obtained for the unstressed and 0.4% strain conditions by using an exponential law based on the work of Nakada et al. [18] and Karlsen [19], resulting in the correlation shown in Fig. 7. From this correlation, φ_γ at 50% and 80% of the YS is estimated as 7.5% and 4.4%, respectively.

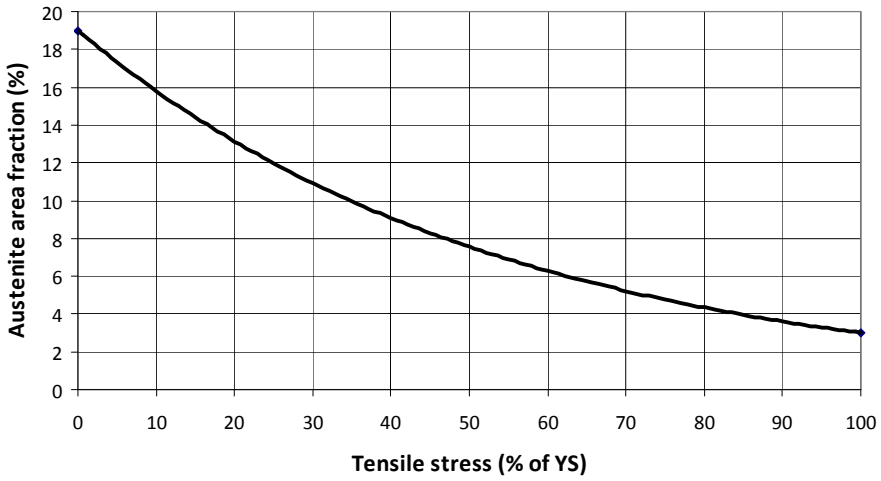

Figure 7. *Austenite area fraction as a function of tensile stress in 13% Cr super martensitic stainless steel.*

Experimental results

Effective hydrogen diffusion coefficient

Effective hydrogen diffusion coefficient data obtained for three replicate 13% Cr SMSS specimens in the as-received condition (zero stress) and under applied stress are shown in Fig. 8. D_{eff} for the as-received condition was in the range $1.7 \cdot 10^{-9}$ to $4.05 \cdot 10^{-9}$ cm^2/s and in agreement with the previously reported values [17] for this type of steel. The data for the replicate specimens showed significant scatter with an average standard deviation of 112%. However, judging from the individual trends in the data for each replicate specimen, as well as the average for the replicate specimens, hydrogen diffusion coefficient appeared to increase moderately with tensile stress.

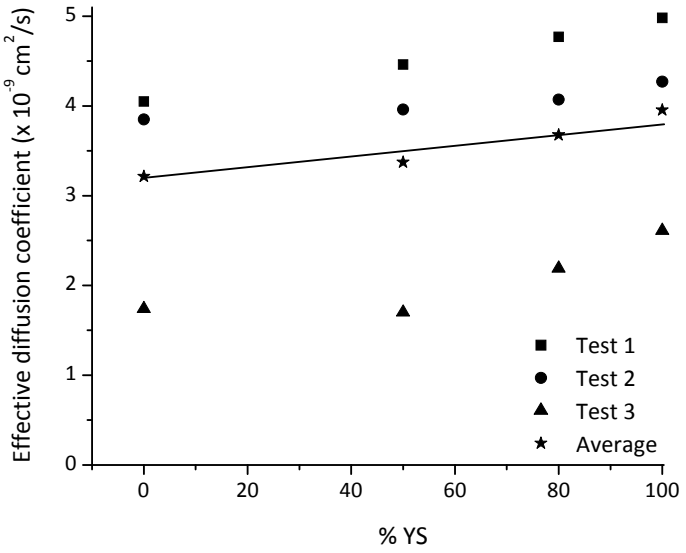

Figure 8. *Effective hydrogen diffusion coefficient as a function of tensile stress in 13% Cr super martensitic stainless steel.*

Sub-surface hydrogen concentration

The sub-surface hydrogen concentration, calculated using Eq. 1, is shown in Fig. 9 as a function of tensile stress. C_0 values were in the range 10 to 15 ppm. However, the average value for the replicate specimens did not vary appreciably with tensile stress, and it was about 11 $\pm$ 3 ppm. This value is four orders of magnitude larger than the results reported by Hinds et al. [17] for a similar type of steel. These authors used the lattice diffusion coefficient of pure iron to estimate the sub-surface hydrogen concentration.

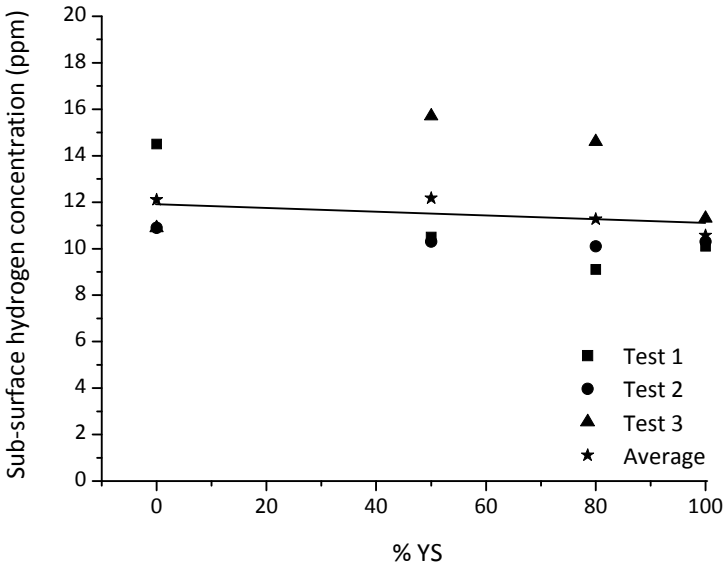

Figure 9. Effective s*ub-surface concentration of hydrogen as a function of tensile stress in 13% Cr super martensitic stainless steel.*

Discussion

The effective diffusion coefficient of 13% Cr SMSS appeared to increase slightly with increasing applied tensile stress. However, taking into account the data scatter in the range ±50%, which is common in such measurements [14], the change is not significant. It can be concluded therefore that D_{eff} for this type of steel for applied YS in the range 0 to 100% was $(3.5 \pm 1.3) \cdot 10^{-9}$ cm^2/s at 20°C. Since the trends in D_{eff} with increasing applied stress for the replicate specimens were nearly parallel without any cross-overs, the scatter in the data is attributed to slight differences in the microstructure and residual stresses present in the replicate specimens. These may vary with respect to position in the plate from which the samples were cut. Differences may also be introduced as a result of machining in sample preparation [20].

A slight increase in the hydrogen diffusion coefficient with tensile stress can be attributed to the reduction in the volume fraction of austenite phase when 13% Cr SMSS undergoes deformation. The mechanism of deformation-induced martensitic transformation has been well studied and described by Olson and Cohen [21, 22]. A similar decrease in the retained austenite fraction with application of strain in martensitic stainless steel was also reported by Nakada et al. [18] and Karlsen [19]. Moreover, an increase in the hydrogen diffusion with an increase in the fraction of martensitic phase was reported by Perng and Altstetter [23] for unstable AISI 301 and AISI 304 austenitic stainless steels undergone deformation. Hydrogen diffusion is much faster in martensite (diffusion coefficient is in the order of 10^{-8}…10^{-9} cm^2/s) than in austenite (diffusion coefficient is in the order of 10^{-12}…10^{-13} cm^2/s) [24]. The EBSD analysis suggests that approximately 85% of retained austenite transformed into martensite after 0.4% strain which lead to a slight increase in the hydrogen diffusion coefficient.

The scatter in the C_0 values, which is actually much smaller than the scatter in the D_{eff} data, are attributed to irreproducible surface finish and surface conditions during the diffusion experiments. The test section could not be polished because of its indented geometry. Exposure to NaCl solution at alternating potentials of -1050 and -550 mV vs. Ag/AgCl may have altered the properties of the oxide during each flux transient. Although the surface should not corrode in this potential range [25], the state of passivity is expected to change. The apparent lack of change in C_0 with applied tensile stress is in conflict with the results for pure iron and ferritic steels [8, 11]. However, these results are not directly comparable with the present data because of the obvious difference in the microstructure. The present results were moreover based on the correction for the area fraction of the austenite phase, which is an additional source of uncertainty.

Conclusions

1. The average effective hydrogen diffusion coefficient of 13% Cr SMSS is $3.5 \pm 1.3 \cdot 10^{-9}$ cm^2/s at 20°C in the presence of 0% to 0.4% strain. A slight increase in D_{eff} is indicated with increasing strain, attributable to the reduction in the volume fraction of the austenite phase

2. The sub-surface hydrogen concentration did not vary with tensile stress. The average value of the sub-surface hydrogen concentration was around 11 ± 3 ppm.

References

[1] S. Huizinga et al., Proceedings of the NACE International Corrosion Conference and Exposition, **2006**, Paper No.06145.

[2] P. Woolin and W. Murphy, Proceedings of the NACE International Corrosion Conference and Exposition, **2001**, Paper No.01018.

[3] S. Olsen et al., Proceedings of the NACE International Corrosion Conference and Exposition, **2001**, Paper No.01091.

[4] S.P. Lynch, Proceedings of the NACE International Corrosion Conference and Exposition, **2007**, Paper No.07493.

[5] R. Johnsen, B. Nyhus, S. Wästberg, Proceedings of the International Conference on Ocean, Offshore and Arctic Engineering (OMAE), **2009**, Paper No.79325.

[6] DNV-RP-F112 “Design of duplex stainless steel subsea equipment exposed to cathodic protection”.

[7] R. Johnsen, B. Nyhus, S. Wästberg, Proceedings of EuroCorr **2008** International Conference, Paper No.1090.

[8] V. Olden, C. Thaulow, R. Johnsen, Materials and Design 29 (10), **2008**, pp. 1934-1948.

[9] Y. Huang et al., ISIJ International 43 (4), **2003**, pp. 548-554.

[10] S. S. Chen et al., Journal of Materials Science 39, **2004**, pp. 67-71.

[11] M. Kurkela et al., Scripta Metallurgica 16, **1982**, pp. 455-459.

[12] L.-C. Hwang and T.-P. Perng, Materials Chemistry and Physics 36, **1994**, pp. 231-235.

[13] S. M. Hesjevik and S. Olsen, Preccedings of NACE Corrosion **2004** International Conference, Paper No.04545.

[14] M.A.V Devanathan and Z. Stachurski, Proc. Royal Society (A) 270, 1340, **1962**, p. 90.

[15] ISO 17081:**2004**, ”Method of measurement of hydrogen permeation and determination of hydrogen uptake and transport in metals by an electrochemical technique”.

[16] K. Kiuchi and R.B. McLellan, Acta Metall. 31 (7), **1983**, pp. 961-984.

[17] G. Hinds et al., Corrosion 61 (4), **2005**, pp. 348-354.

[18] N. Nakada et al., The 3rd International Conference of Advanced Structural Steels, Gyeongju, Korea, August 22-24, **2006**.

[19] M. Karlsen, Ph.D. Thesis, NTNU, **2009**.

[20] M. Mouanga, P. Bercot, J. Takadoum, Corr. Sci. 52, **2010**, pp. 2010-2014.

[21] G.B. Olson and M. Cohen, J. of Less-Common Met. 28, **1972**, p. 107-118.

[22] G.B. Olson and M. Cohen, Metallurgical Transaction 13A, **1982**, pp. 1907-1914.

[23] T.-P. Perng and C. J. Altstetter, Acta Metall. 34 (9), **1986**, pp. 1771-1781.

[24] V. Olden, C. Thaulow, R. Johnsen, Mater. Design 29, **2008**, pp. 1934-1948.

[25] ISO 15589-1:**2003**, ”Petroleum and natural gas industries – cathodic protection of pipeline transportation systems”.